



## THE EFFECT OF EMBEDMENT OF LARGE-SCALED STRUCTURES ON THE STABILITY AGAINST SLIDING DURING STRONG EARTHQUAKE MOTIONS

K. FUKUSHIMA\*, H. IZUMI\*\* and F. MIURA\*\*\*

\* Engineer, Design Planning Dept., Civil Engineering Div., 1-25-1 Nishi-Shinjuku, Shinjuku-ku, Tokyo, 163-06, JAPAN

\*\* Manager, Shinozuka Reserch Institute, JM Bldg, 6-26-4 Shinjuku, Shinjuku-ku, Tokyo 160, JAPAN

\*\*\* Professor, Department of Computer Science and Systems Engineering, Faculty of Engineering, Yamaguchi University, Tokiwadai, Ube 755, JAPAN

### ABSTRACT

Nonlinear seismic response analyses of ground-structure interaction systems were performed by using the finite element method which took into account the material nonlinearity of soil and, sliding and separation phenomena at the contact surface between the structure and soil. In order to evaluate the safety against sliding, the factor of safety against sliding from the stresses of joint elements that were arranged along the contact surface. A parametric study was performed by using a rectangular structure of 45m in width and 40m in height by changing the depth of the embedment of structure and the thickness of the surface layer. Three strong accelerograms which have different predominant frequencies were used as input motions. From the parametric study, it was found that the factor of safety against sliding depended on both the depth of the embedment and the thickness. There was a general tendency that the thinner the surface layer, the lower the factor. As for the depth of the embedment, there was an optimal depth which gave the highest factor of safety.

### KEYWORDS

Soil-structure interaction, nonlinear analysis, dynamic stability, safety against sliding, finite element method, embedment of structure.

### INTRODUCTION

Important large-scale structures such as abutment of long suspension bridges, power plant structures and so on must be safe even when they are subjected to strong earthquake motions. They are generally built on firm rock foundation, however, they are at times built on alluvial ground. In such a case, the foundation of the structure must be embedded into ground to obtain dynamic stability especially against sliding. It is, therefore, necessary and important to evaluate the effectiveness of the embedment. In spite of the importance, there are only a few studies which investigated the effect. From this point of view, the purpose of this study is to quantitatively investigate in detail the effectiveness of the embedment of structure in the ground against sliding.

We performed the nonlinear seismic response analyses of alluvial ground-structure interaction systems by using the finite element method which took into account the material nonlinearity of soil and, sliding and separation phenomena at the contact surface between the ground and the structure. In order to evaluate the safety

against sliding, we calculated the factor of safety (we use the term, Total Safety Factor, i.e., T.S.F., in this study) from the stresses of joint elements that were arranged along the contact surface. We conducted a parametric study using a rectangular structure of 45m wide and 40m high by changing the depth of the embedment of structure in the ground from 0m to 40m. The thickness of the surface layer was also changed from 50m to 100m. Three strong accelerograms which have different predominant frequencies were used as input motions.

## ANALYSIS METHOD AND ANALIZED MODELS

Figure 1 shows the structure-ground interaction system which was analyzed in this study. The width of the structure is 45m and the height is 40m. Modified joint elements (Toki *et. al.*, 1985) are arranged along the contact surface between the structure and ground. The material constants of the structure, ground and joint elements are shown in the figure. The bottom of the ground is fixed and the consistent viscous boundary based on the principle of virtual work (Miura *et. al.*, 1989) are introduced at both side-boundaries of the ground in order to absorb the radiation wave energy. The position of the boundaries, i.e., the distance of the boundary from the structure was determined based on the study conducted by Iwatate (1991). The depths of the embedment of structure into the ground are 0m, 10m, 20m, 30m and 40m and they are called Model 0/4, Model 1/4, Model 2/4, Model 3/4, and Model 4/4, respectively. Fundamental natural frequencies of these models are 0.79Hz, 0.82Hz, 0.85Hz, 0.88Hz and 0.92Hz, respectively. Pairs of horizontal and vertical strong earthquake motions were used as input accelerograms. They are the El Centro NS and UD components (Kern County EQ. 1945), The Hachinohe EW and UD components (Tokachi-oki EQ., 1968) and the Kaihoku NS and UD components (Miyagiken-oki EQ., 1978). Predominant frequencies of three horizontal components are 1.51Hz, 0.98Hz and 2.88Hz, respectively. The predominant frequency of the Hachinohe EW component, 0.98 Hz, is close to the fundamental natural frequencies of the five soil-structure interaction models.

The equation of motion for the interaction system was solved by using the Newmark's  $\beta$  method ( $\beta = 1/4$ ). Nonlinearities such as material nonlinearity of soil and geometrical nonlinearity of sliding and separation phenomena at the contact surface were solved by the load transfer method. It is one of the iterative methods. The factor of safety against sliding of the whole structure (Total Safety Factor; T.S.F.) was obtained from the stresses induced in joint elements that were used to model the contact surface by the following equation.

$$T. S. F. = \left| \frac{\sum \tau_{yi} A_i}{\sum \tau_i A_i} \right|_{\min} . \quad (1)$$

Where,  $\tau_{yi}$  is the yield shear stress of the nodal pair,  $i$ , of a joint element,  $A_i$  is the sharing area of the nodal pair,  $i$ ,  $\tau_i$  is the induced shear stress which is given by eq.(2)

$$\tau_{yi} = C_i + \sigma_n \tan \phi_i \quad (2)$$

in which,  $C_i$  and  $\phi_i$  are the cohesion and angle of friction at the nodal pair  $i$ .  $\sigma_n$  is the time dependent normal stress.

## ANALYSIS RESULTS

### The effect of vertical excitation

There was no detailed investigation of the effect of vertical excitation on the sliding stability of a structure despite the importance of the investigation that has been well recognized. Three different combinations of horizontal and vertical accelerograms were employed as input motions. They are:

- i ) Horizontal input motion only. The maximum amplitude at the surface of free field was adjusted to be 300 gal. The symbol in the following figures is  $\blacktriangle$  or  $\triangle$ . We call this input as "Input 1".
- ii ) Horizontal input motion with the maximum amplitude of 300gal and vertical input motion with the maximum

amplitude of the same amplification ratio to the original acceleration as that of the horizontal motion. We call this combination as "Input 2". The symbol is ● or ○.

iii) Horizontal and Vertical input motions with the maximum amplitudes of 300 gal, "Input 3". The symbol is ■ or □.

The input motions above were converted from the accelerograms recorded at the ground surface to those at the fixed base of the model through the deconvolution procedure.

Figure 2 shows the horizontal maximum responses at the top of the structure (Top) and at the bottom of the structure (Bottom). Figure (a) is the maximum response accelerations, (b) the maximum response velocities and (c) the maximum response displacements. The effect of vertical input motions cannot be observed from these figures. The maximum response values reduce with the increment of the magnitude of embedment. The maximum responses in vertical direction are shown in Fig.3. As expected, there are differences in the maximum responses in accordance with the magnitude of the vertical input motions. As eq. (2) means, the yield shear stress,  $\tau_y$ , is the function of the normal stress,  $\sigma_n$ , of the joint element which is expected to be strongly dependent on the vertical excitation because the contact surface is horizontal, therefore,  $\tau_y$  is also expected to be dependent on the vertical excitation. This leads to the dependence of T.S.F. on the vertical excitation.

Figure 4 shows the obtained T.S.F.s. Figure (a) compares T.S.F.s obtained from the El Centro accelerograms, (b) from the Hachinohe accelerograms and (c) from the Kaihoku accelerogram excitations. From these figures, it is found that although there is a little difference in T.S.F.s with respect to vertical input motion for Hachi-nohe cases (Fig.2 (b)), there is no difference in T.S.F.s for other excitations. This implies that the vertical excitation does not affect the sliding stability of the structure even if the magnitude of the amplitude of the vertical input motion is as large as that of the horizontal one.

One more important thing can be recognized from these figures. The maximum T.S.F.s are obtained for Model 1/4 for all three accelerograms. This indicates that there exists an optimal magnitude of embedment. To understand the independency of T.S.F. on vertical excitations and the existence of the optimal magnitude of embedment, we investigated the forces acting on the structure during the excitation. Figure 5 shows the forces acting on the structure. Equilibrium conditions in horizontal and vertical directions exist in every moment during the excitation as follows.

$$F_x + S + R_L + R_R = 0 \quad (\text{Horizontal direction}) \quad (3)$$

$$F_y + N + S_L + S_R - W = 0 \quad (\text{Vertical direction}) \quad (4)$$

Where,  $F_x$  and  $F_y$  are inertia forces in horizontal (x) and vertical (y) directions at the center of gravity of the structure. S and N are the shear force and the normal force at the base of the structure.  $R_L$  and  $R_R$  are the normal forces acting on the side walls of the structure.  $S_L$  and  $S_R$  are the shear forces acting on the side walls of the structure. Subscripts L and R for these forces mean "Left" and "Right", respectively. W is the weight of the structure.

The magnitudes of these forces at the moment that the T.S.F. is obtained, i.e., the safety against sliding becomes minimum, are summarized in Figs. 6(a) and (b). Figure (a) is for the horizontal equilibrium and (b) for the vertical equilibrium for the El Centro excitations. From these figures, no difference is observed in all forces despite the difference of vertical excitations. No difference in these forces results in no difference in T.S.F. irrespective to vertical excitations. Broken lines in Fig. 6 (a) shows the magnitude of initial force acting on the side walls of the structure due to the initial earth pressure. The inertia force,  $F_x$ , gradually decreases as the increment of embedment, which is consistent with the tendency of the maximum response acceleration shown in Fig. 2 (a). The magnitude of the normal forces,  $R_L$  and  $R_R$ , increases with the increment of embedment, and the sum of these forces gradually increase with the increment of the embedment. The balance of these forces which is given by eq. (3) results in the increment of the magnitude of S with the increment of embedment except for zero embedment (Model 0/4). For Model 0/4, in case of zero embedment,  $R_L$  and  $R_R$  do not exist and therefore S balances with  $F_x$ . It can be noted that the tendency of curve S with respect to the magnitude of embedment resembles that of the curves of T.S.F. shown in Fig. 4. On the other hand, forces

vertically acting on the structure do not change as shown in Fig. 6 (b) as could be seen for horizontal forces in Fig. 6 (a). Roughly, T.S.F. is proportional to the ratio of S/N. While N is almost constant for all embedment, S changes with the magnitude of the embedment and is minimum at 1/4. This results in the existence of the optimal depth of the embedment.

#### The effect of material nonlinearity of soil

Soil behaves as nonlinear material when subjected to strong ground motion. Therefore, the effect of material nonlinearity on T.S.F. was investigated by assuming that the soil was an elasto-perfect plastic body. Figure 7 shows the comparison of the results from the nonlinear material analyses and those from the linear material analyses. Figure (a) compares T.S.F.s., (b) horizontal displacements at the center of gravity of the structure (sway) and (c) the inclination angles (rocking). These analyses were performed for the model with 100m surface layer and for the E1 Centro input motions. T.S.F.s obtained from the nonlinear material analyses are higher than those obtained from the linear material analyses (Fig.7 (a)). There is no difference in sway responses (Fig.7(b)). The inclination angles obtained from nonlinear material analyses are slightly smaller than those obtained from the linear material analyses (Fig.7(c)). From these results the discussion for linear material analyses is conservative. Therefore, the discussion is done for the linear material analyses in the next section.

#### The effect of the thickness of the surface layer.

In the previous sections the analyses were performed by fixing the thickness of the surface layer to be 100m. As easily expected, T. S. F. s would be affected by the thickness of the surface layer because the distribution of the stresses induced in the layer depend on the thickness. From this point of view, we performed the analyses by changing the thickness from 50m to 100m with the interval of 10m. Figure 8 summarizes the obtained T. S. F. s. There are two general tendencies; first, T.S.F.s. are higher for the thicker layer for the same magnitude of embedment; second, highest T.S.F.s are obtained when the embedment is 1/4 for the same thickness. The reason for the second tendency has already been discussed in the previous section.

In order to understand the first tendency, we examined the distribution of horizontal displacement along the depth. Figure 9 shows the distributions. It is clear from these figures that the changes in magnitude of the displacement near the ground surface are smaller for the thicker layers. To discuss this tendency more quantitatively, we introduced a nondimensional parameter,  $P_h$ , which is defined as follows.

$$P_h = (u_s - u_B) / H_s \quad (5)$$

Where,  $u_s$  is the horizontal displacement at the surface of the free field and  $u_B$  is the horizontal displacement of the free field at the depth which corresponds to the base of the structure.  $H_s$  is the depth of the embedment as shown in Fig.10(a). Shear force induced at the structural base, S, are summarized with respect to the parameter,  $P_h$ , in Fig.10(b). There is a good correlation between S and  $P_h$ , which means that S would be evaluated from  $P_h$ , in other words, only from the free field analyses without performing the analyses of soil-structure interaction system. Furthermore, we tried to introduce another nondimensional parameter,  $P_v$ , which is defined as follows (see Fig.11(a)).

$$P_v = H_s / H_g \quad (6)$$

Where,  $H_g$  is the thickness of the surface layer. The relationship between S and  $P_v$  are summarized in Fig. 11(b). There is also a good correlation between the two. This implies that S would be evaluated just from the geometric parameters  $H_s$  and  $H_g$  without any dynamic analysis from even that of free field. Once the shear force induced at the bottom of the structure, S, is obtained the factor of safety (F.S.) against sliding is obtained by using the normal force N which is nearly equal to the weight of the structure, W, as follows.

$$F.S. = (C + N \tan \phi) / S \doteq (C + W \tan \phi) / S \quad (7)$$

Where, C and  $\phi$  are the cohesion and the angle of friction at the contact surface between the structural base and soil.

## CONCLUSIONS

We performed the parametric study of nonlinear seismic response analyses of ground-structure interaction systems by using the finite element method which took into account the material nonlinearity of soil and sliding and separation phenomena at the contact surface between the structure and soil. From the parametric study we obtained the following conclusions.

- (1) Total Safety Factor of the whole structure, T.S.F., depends on both the depth of the embedment of structure and the thickness of the surface layer.
- (2) There was a general tendency that the thinner the surface layer, the lower the T.S.F..
- (3) There was an optimal depth which gives the highest T.S.F.. For the deeper embedment, T.S.F. decreases in increment of embedment. The reason why the deeper embedments give lower T.S.F.s was that the increment of active dynamic earthpressure acting on the side walls of the structure led to the increment of shear force at the structural base.
- (4) In order to estimate the shear force at the structural base, we introduce two nondimensional parameters. First one is the function of the free field displacements and the depth of the embedment and the second one is the function of the depth of the embedment and the thickness of the surface layer. Both parameters have good correlation with the shear force. This implies that it's a possibility to estimate of the factor of safety of a structure against sliding without any dynamic response analyses of the interaction system.

## REFERENCES

- Iwatate, T. (1991). Estimation method of seismic response of embedded structure-soil interaction system, *Report of Central Research Institute of Electric Power Industry*, U20 (in Japanese).
- Miura, F. and H. Okinaka (1989). Dynamic analysis method for 3-D soil-structure interaction systems with the viscous boundary based on the principle of virtual work. *Proc. of JSCE*, No.404/I-11, 395-404(in Japanese).
- Toki, K. and F. Miura (1985). Simulation of a fault rupture mechanism by a two-dimensional finite element method. *J. Phys. Earth*, 33, 485-511.

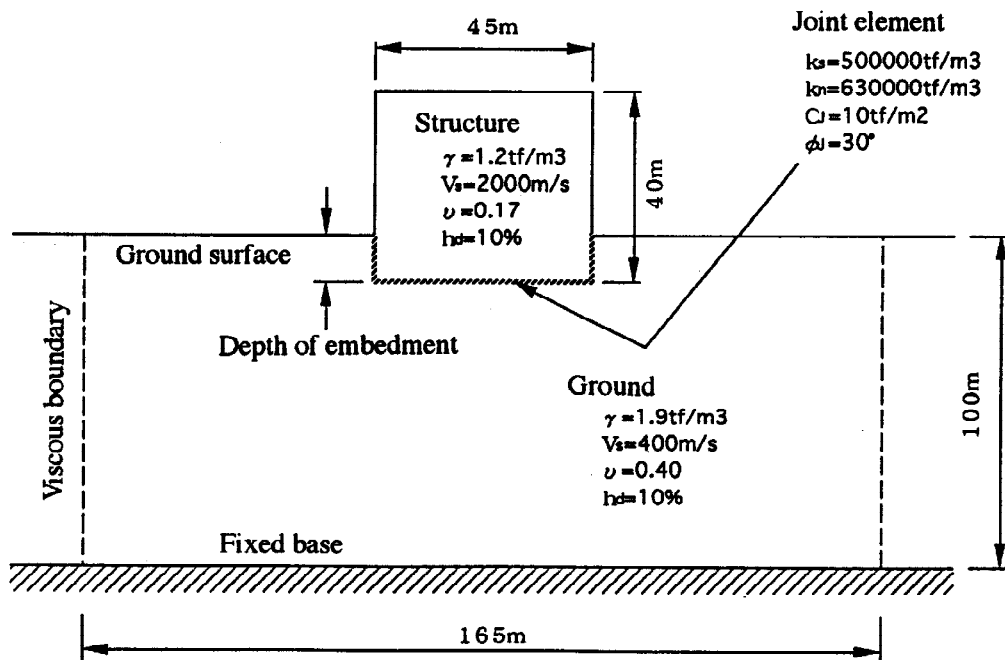


Fig.1 Analyzed structure-ground-interaction model.

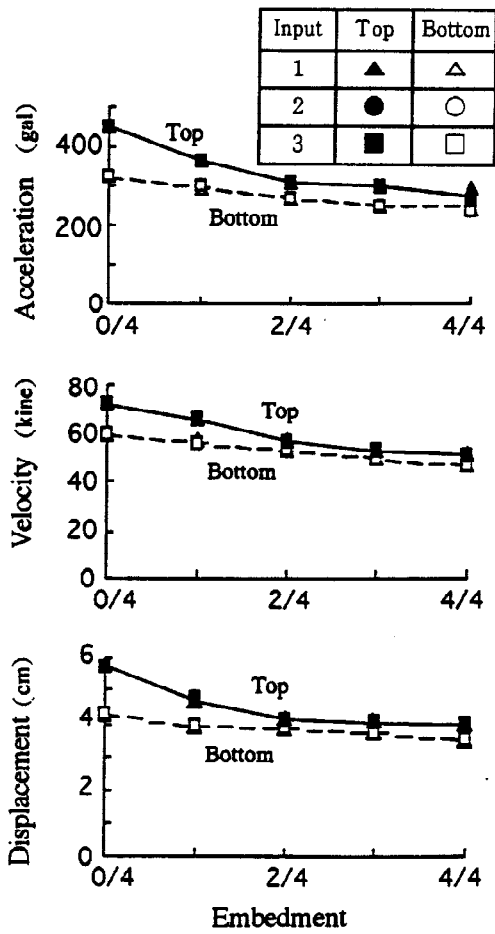


Fig.2 Horizontal maximum responses

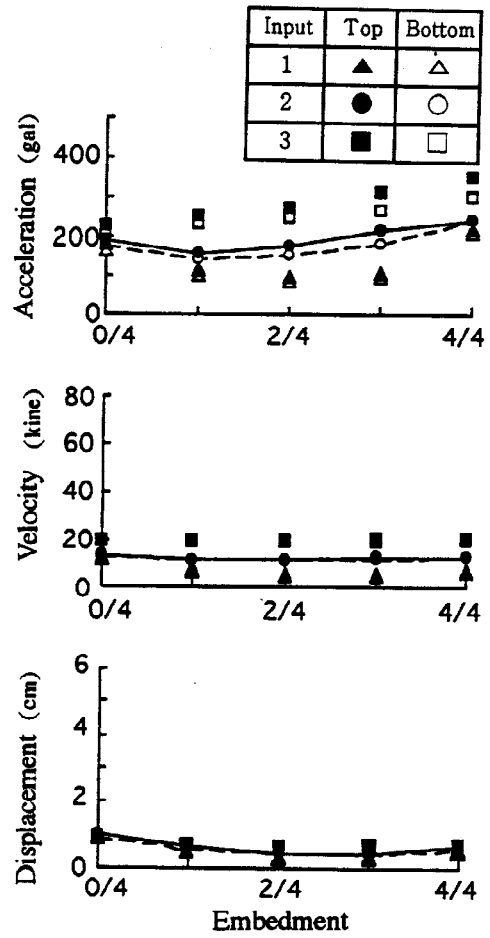
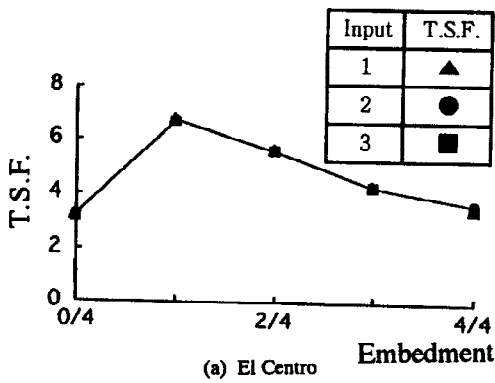
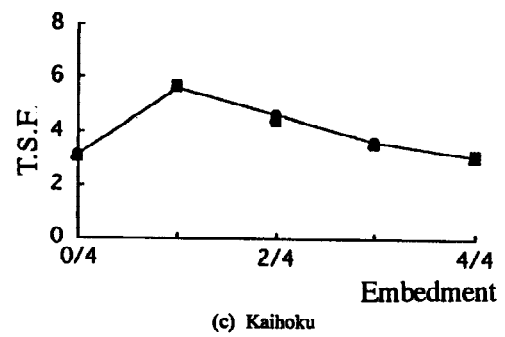


Fig.3 Vertical maximum responses

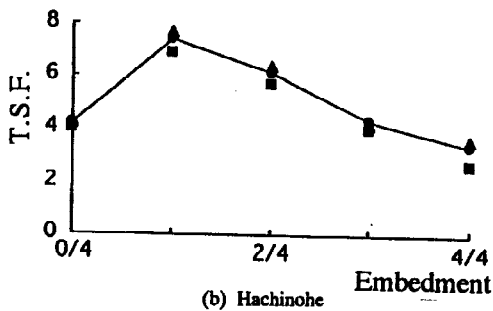


(a) El Centro



(c) Kaihoku

Fig.4 Relationship between T.S.F. and the embedment



(b) Hachinohe

Fig.4 Relationship between T.S.F. and the embedment

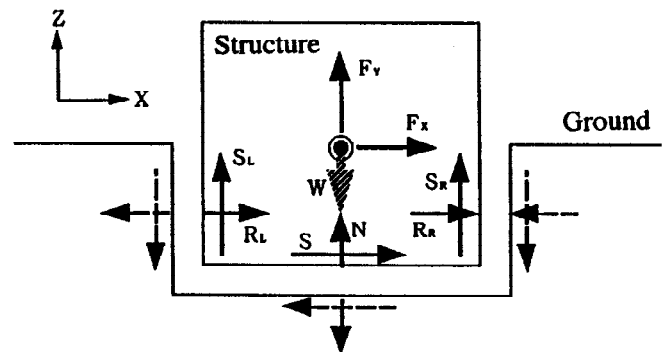


Fig.5 Notations of forces



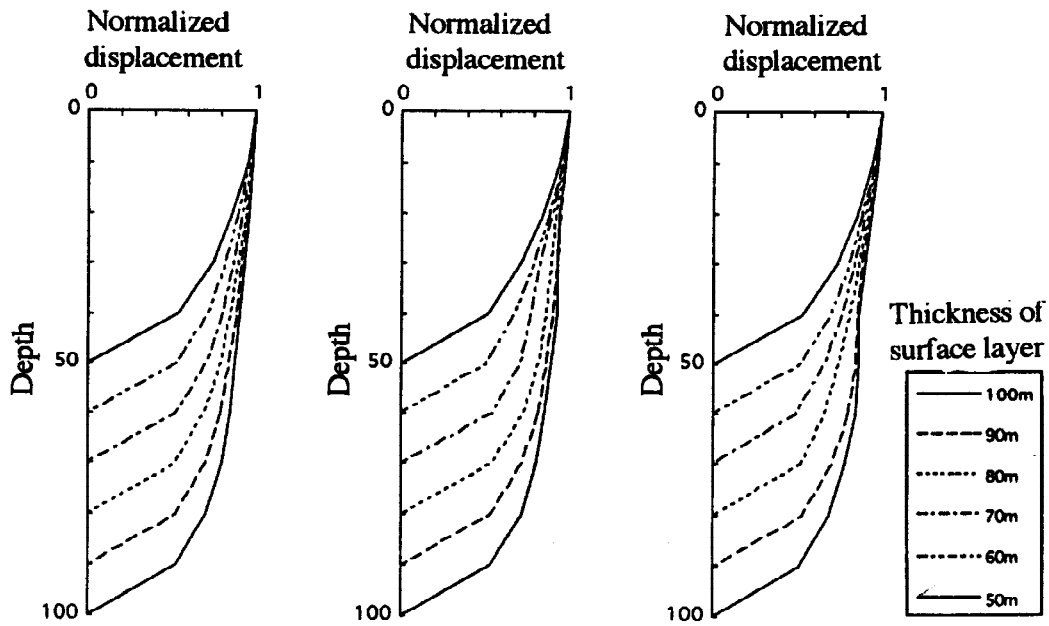


Fig.9 Distribution of normalized horizontal displacement in depth

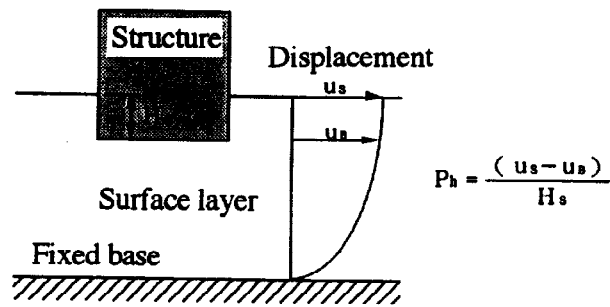


Fig.10 (a) Definition of  $P_h$

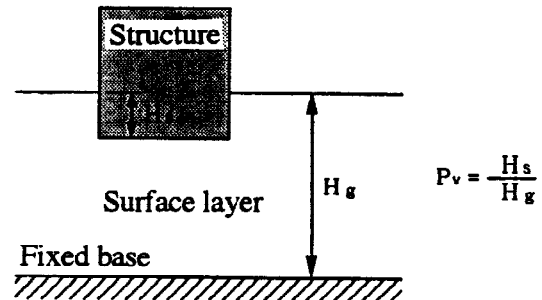


Fig.11 (a) Definition of  $P_v$

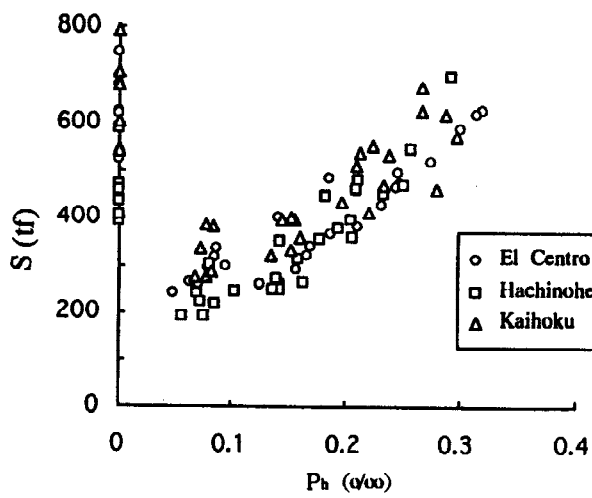


Fig.10 (b) Relationship between  $P_h$  and  $S$

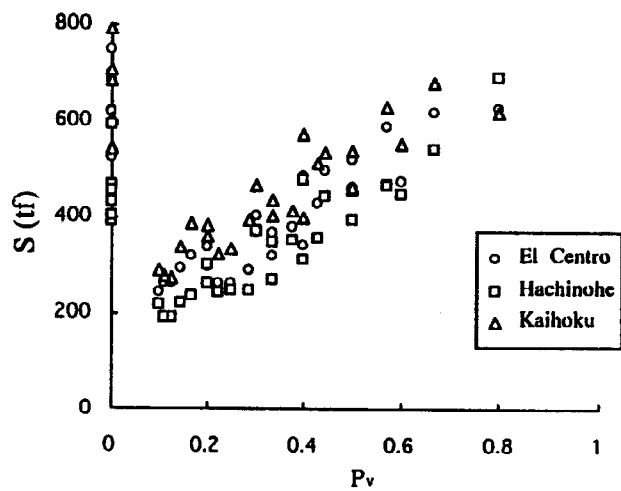


Fig.11 (b) Relationship between  $P_v$  and  $S$